

Genetic Analysis of Ephrin-A2 and Ephrin-A5 Shows Their Requirement in Multiple Aspects of Retinocollicular Mapping

David A. Feldheim,* Young-In Kim,*^{||}
Andrew D. Bergemann,*[#] Jonas Frisén,[†]
Mariano Barbacid,[‡] and John G. Flanagan*[§]

*Department of Cell Biology and
Program in Neuroscience
Harvard Medical School
Boston, Massachusetts 02115

[†]Department of Cell and Molecular Biology
Medical Nobel Institute
Karolinska Institute
S-171 77 Stockholm
Sweden

[‡]Centro Nacional de Investigaciones
Oncológicas Carlos III
Instituto de Salud Carlos III
28220 Majadahonda
Spain

Summary

Ephrin-A2 and -A5 are thought to be anteroposterior mapping labels for the retinotectal/retinocollicular projection. Here, gene disruptions of both these ephrins are characterized. Focal retinal labeling reveals moderate map abnormalities when either gene is disrupted. Double heterozygotes also have a phenotype, showing an influence of absolute levels. In vitro assays indicate these ephrins are required for repellent activity in the target and also normal responsiveness in the retina. In double homozygotes, anteroposterior order is almost though not completely lost. Temporal or nasal retinal labelings reveal quantitatively similar but opposite shifts, with multiple terminations scattered widely over the target. These results indicate an axon competition mechanism for mapping, with a critical role for ephrins as anteroposterior topographic labels. Dorsoventral topography is also impaired, showing these ephrins are required in mapping both axes.

Introduction

Axon projections in the vertebrate nervous system are typically organized as topographic maps, with nearest neighbor relationships of the projecting neurons maintained in their connections within the target. In this manner, the spatial content of information can be preserved as it is transferred from one area to another. For example, retinal axons project topographically to their targets in the brain, allowing visual images to be transferred in a spatially intact form.

[§]To whom correspondence should be addressed (e-mail: flanagan@hms.harvard.edu).

^{||}Present address: Departments of Medicine and Nutritional Sciences, University of Toronto, Toronto, Ontario, Canada, M5S 1A8.

[#]Present address: Department of Pathology, Mount Sinai School of Medicine, New York, New York 10029.

A prevailing model for the mechanism of topographic map formation was proposed by Sperry (1963) in the chemoaffinity theory. This theory proposes that there are labels in gradients across the projecting and target fields and that axons find their correct location by matching up the labels. Evidence supporting this theory came from a wide variety of studies over a period of decades, involving tissue grafting and ablation, axon tracing, and in vitro axon guidance assays. The major model system used for these studies has been the visual projection from the retina to the tectum or to its mammalian equivalent, the superior colliculus (SC) (reviewed by Drescher et al., 1997; Flanagan and Vanderhaeghen, 1998; O'Leary et al., 1999).

In the last few years, ephrins and their Eph receptors have been identified as likely candidates for graded labels of the type predicted by Sperry. In chick, ephrin-A2 and ephrin-A5 are expressed in overlapping posterior > anterior gradients across the tectum (Cheng et al., 1995; Drescher et al., 1995), while the receptor EphA3 is expressed in a corresponding temporal > nasal gradient across the retina (Cheng et al., 1995). The ligands are sufficient to repel chick retinal axons with a topographically specific preference for temporal axons, as shown by assays in vitro (Nakamoto et al., 1996; Monschau et al., 1997; Feldheim et al., 1998) and gain-of-function experiments in vivo (Nakamoto et al., 1996). In addition to functions in the target, in vitro assays and gain-of-function experiments have led to the proposal that ephrin-A2 and -A5 may also act in the retina, downregulating functional receptors in nasal axons (Hornberger et al., 1999).

Studies in the mouse support a similar function for ephrins. Graded expression patterns comparable to those in chick are seen in mouse (Cheng and Flanagan, 1994; Flenniken et al., 1996; Marcus et al., 1996; Zhang et al., 1996; Frisén et al., 1998), though with EphA5 rather than EphA3 in a gradient across the retinal ganglion cell layer (Feldheim et al., 1998). In vitro assays show topographically specific repulsion of mouse retinal axons by ephrin-A2 and -A5 (Feldheim et al., 1998). Moreover, loss-of-function studies by gene disruption showed that ephrin-A5 is required for normal mapping, with temporal axons terminating more posteriorly than normal (Frisén et al., 1998). However, map topography still appeared largely intact, suggesting either that ephrins may not have a major role in mapping or that there could be partial redundancy of ephrin-A2, ephrin-A5, and perhaps other ephrins.

While previous studies support the idea that ephrins are topographic labels, other aspects of mapping remain poorly understood. As pointed out by Gierer (1981), it seems hard to account for topographic mapping in terms of only a single type of gradient per axis. For example, if there were only a repellent gradient, presumably all axons would simply be repelled to one end of the target. It was therefore proposed that there may be two opposing gradients, for example a repellent and an attractant, with each axon identifying its correct place as the point where the opposing forces cancel out (Gierer,

1981). Such dual-gradient models have been considered a likely explanation of map formation in recent years (Drescher et al., 1997; Flanagan and Vanderhaeghen, 1998; O'Leary et al., 1999). However, alternative mechanisms, such as axon-axon competition for space in the target, could also explain the ability of axons to distribute throughout the map (Prestige and Willshaw, 1975; Fraser and Hunt, 1980).

Another issue that remains poorly understood is how a map forms in two dimensions. It has generally been assumed that there are distinct anteroposterior and dorsoventral mapping axes, with separate labels for each (Drescher et al., 1997; Flanagan and Vanderhaeghen, 1998; O'Leary et al., 1999). However, axon guidance assays have so far identified only anteroposterior labels (Walter et al., 1987). Intriguingly, ephrin-B ligands and EphB receptors are expressed in dorsoventral gradients, and although it is not yet clear if their exact locations and functional properties are appropriate, a role in dorsoventral mapping seems very plausible (Holash and Pasquale, 1995; Kenny et al., 1995; Marcus et al., 1996; Braisted et al., 1997). It is worth noting, however, that despite a widespread assumption of two distinct mapping axes, there is no direct evidence to show that mapping must be specified by independent anteroposterior and dorsoventral labels.

We describe here a genetic loss-of-function analysis of *ephrin-A2*^{-/-} and *ephrin-A5*^{-/-} mutants, as well as double homozygotes and double heterozygotes. These two ephrins are shown to have overlapping but distinct functions in map formation. In the double homozygote, axons labeled at temporal or nasal extremes of the retina show approximately equal but opposite shifts in the SC, providing strong support for a model for map specification based on axon competition. Mix-and-match in vitro assays using mutant retina or tectum show that the ephrins act in both projecting and target areas. Finally, the double mutants have abnormalities along the dorsoventral axis, revealing a previously unsuspected role of ephrin-A2 and -A5 in specification of both axes.

Results

ephrin-A2 and *ephrin-A5* Single Mutant Mice Have Moderate Defects Indicating Overlapping but Distinct Functions

To test whether ephrin-A2 is required for proper retinocollicular development, we used homologous recombination in ES cells to generate mice with a disruption in the *ephrin-A2* gene. A *neo* selection cassette with stop codons in all three reading frames was inserted after amino acid 66 in the ephrin-A2 sequence. Since this is just upstream of the first of the four cysteines that form a conserved motif throughout the ephrin family, and since most of the extracellular domain is encoded in a single exon (Cerretti and Nelson, 1998), the mutated gene is likely to be a null allele. The mutation was confirmed by Southern blotting, PCR amplification of genomic DNA, and RT-PCR of RNA from wild-type and *ephrin-A2*^{-/-} mice (see Experimental Procedures). *ephrin-A2*^{-/-} mice reach adulthood, are fertile, and showed no gross morphological defects.

To assess the effects of *ephrin-A2* gene disruption

on retinocollicular mapping, a focal injection of Dil was made in one retina followed by examination of the contralateral midbrain. When temporal axons of *ephrin-A2*^{-/-} mice were labeled, an apparently normal arborization was always seen and, in approximately half of the animals (57% penetrance, 12/21 mice), an additional more posterior arborization (Figure 1A). These defects were reminiscent of those reported by Frisén et al. (1998) in *ephrin-A5*^{-/-} mice, where temporal labelings always revealed a normal arborization and in half of the animals tested an additional arborization at a more posterior location within the SC (Figure 1B). However, unlike *ephrin-A5*^{-/-} mutants, the *ephrin-A2*^{-/-} mice showed no abnormal overshooting of axons into the inferior colliculus (IC) during early development of the map, and no axon accumulation could be detected at the SC/IC border of the mature map (data not shown).

We also tested mapping of nasal axons. No defects were found in mapping of nasal axons in *ephrin-A2*^{-/-} mice (Figure 1F). However, we found that *ephrin-A5*^{-/-} mice have a pronounced defect in nasal axon mapping (Figure 1G). In addition to an apparently normal arborization near the posterior end of the SC, most *ephrin-A5*^{-/-} mice (91% penetrance, 20/22 mice) showed an additional arborization in a more anterior location. The ectopic arborizations of the nasal axons were always located in the posterior half of the SC, and the ectopic arborizations of the temporal axons in the anterior half. However, they did not appear to be targeted to any specific ectopic position.

ephrin-A2^{-/-}; *ephrin-A5*^{-/-} Double Mutants Have a Synergistic Phenotype, with Abnormalities of Both Anteroposterior and Dorsoventral Mapping

We next tested *ephrin-A2*^{-/-}; *ephrin-A5*^{-/-} double mutants by focal retinal Dil injections. Typical results are shown in Figure 2, and a summary is in Figure 3. The mapping phenotype was more severe than in either single mutant. The penetrance of abnormal mapping was high for both temporal labelings (85% penetrance, 17/20 mice; Figures 2A, 2C, and 3) and nasal labelings (92% penetrance, 24/26 mice; Figures 2B, 2D, and 3). Temporal and nasal axons were oppositely affected, with temporal axons forming ectopic arborizations in abnormally posterior positions and nasal axons abnormally anterior. In terms of the number of termination zones, single mutants rarely had more than one ectopic arborization (Figure 1), whereas multiple arborizations were typically seen in the double mutants (Figures 2 and 3). Up to five distinct arborizations were seen in the SC of individual double mutants, with the average number being 2.9 ± 1.0 (mean \pm SD) for nasal labelings and 2.5 ± 0.8 for temporal labelings. The ectopic terminations extended over all regions of the anteroposterior mapping axis and did not appear to be targeted to any specific ectopic position. However, they did appear to retain some bias in favor of the correct side of the SC (Figure 3). In contrast to the single mutants, an arborization at the normal location was not always present and often appeared faint relative to the overall labeling at other regions (Figures 2 and 3).

We also assessed mapping in double heterozygote *ephrin-A2*^{+/-}; *ephrin-A5*^{+/-} mice. Temporal axon labelings revealed a phenotype similar to the single mutant

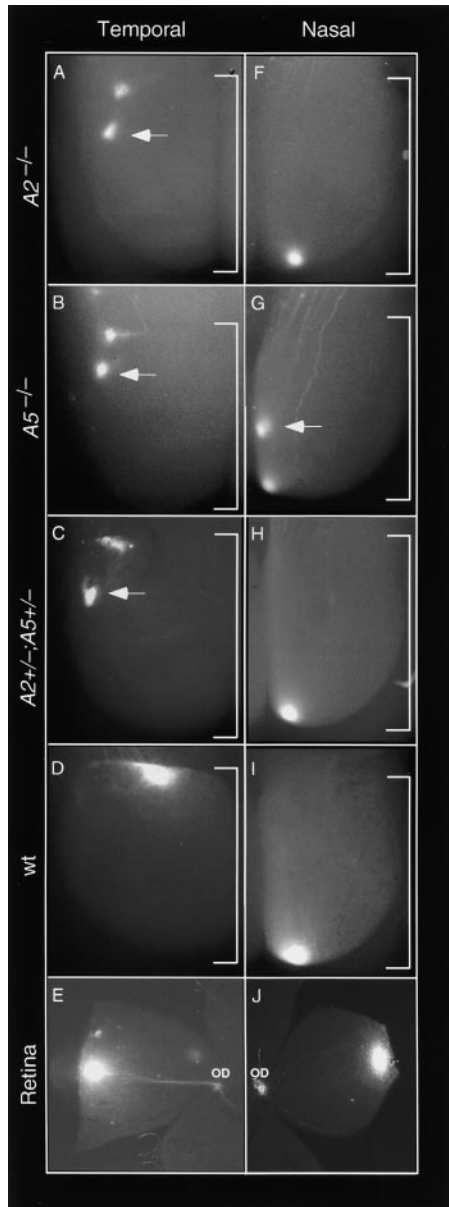


Figure 1. Mapping Abnormalities in the SC of *ephrin-A2*^{-/-} and *ephrin-A5*^{-/-} Single Mutants and *ephrin-A2*^{+/-}; *ephrin-A5*^{+/-} Double Heterozygotes

Retinal axons labeled by focal Dil injection were visualized at P14 by fluorescence microscopy of SC whole mounts. Brackets indicate SC; anterior is at the top.

(A–D) Temporal retinal injections. Mice deficient for *ephrin-A2* (A), *ephrin-A5* (B), and *ephrin-A2*^{+/-}; *ephrin-A5*^{+/-} double heterozygotes (C) show ectopic arborizations posterior to the wild-type arborization site (D).

(F–I) Nasal retinal injections. No nasal axon defects were seen in *ephrin-A2*^{-/-} mutants (F) or *ephrin-A2*^{+/-}; *ephrin-A5*^{+/-} mice (H), whereas *ephrin-A5*^{-/-} mutants (G) show ectopic arborizations anterior to the normal site (I). In addition to ectopic spots, all labelings of these mutants showed a prominent arborization at the normal location. Arrows indicate ectopic arborizations.

(E and J) Temporal or nasal retinal quadrants, respectively, showing typical labeling sites. Axons exit the retina at the optic disc (OD).

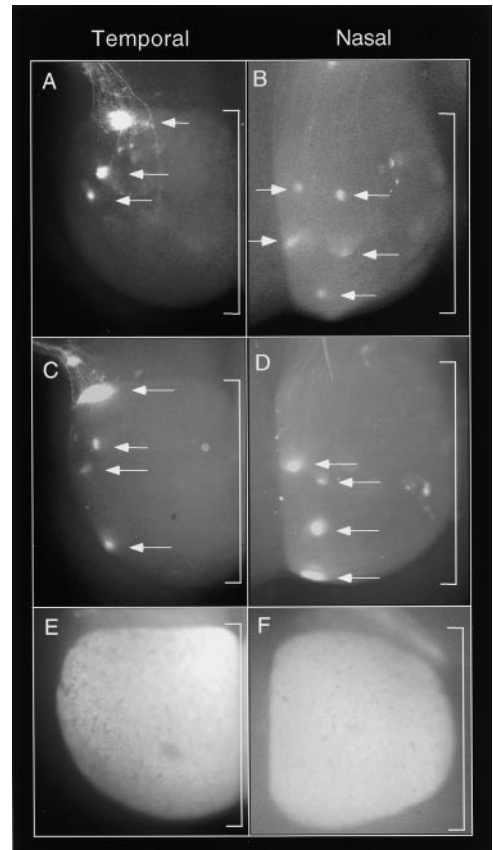


Figure 2. Mapping Abnormalities in *ephrin-A2*^{-/-}; *ephrin-A5*^{-/-} Double Mutants

(A–D) Retinal axons labeled by focal Dil injection were visualized at P14 by fluorescence microscopy of SC whole mounts.

(A and C) Temporal injections.

(B and D) Nasal injections.

Brackets indicate SC; anterior is at the top. Arrows indicate axon arborizations; these were confirmed by their appearance at higher magnification and subsequently by examining sections of the same tissue. Multiple arborizations are seen in the double homozygous mutants, with abnormalities along both anteroposterior and dorsoventral axes. The dorsoventral abnormalities are particularly distinctive in cases where two arborizations have a similar anteroposterior position (B and D).

(E and F) Eye fill with fluoresceinated cholera toxin β subunit to anterogradely label projections throughout the retina. Labeled axons fill the SC in both wild-type and mutant animals.

ephrin-A2^{-/-} or *ephrin-A5*^{-/-} mice, with abnormally posterior ectopic arborizations seen in about half the animals (55% penetrance, 6/11 mice; Figure 1C). When nasal axons were labeled, no abnormalities were seen (0/8 mice; Figure 1H).

In addition to abnormalities along the anteroposterior axis, we were surprised to see that the *ephrin-A2*^{-/-}; *ephrin-A5*^{-/-} double mutants also showed abnormalities in dorsoventral topography (Figure 2). This was particularly obvious in cases where two or more termination zones shared a similar anteroposterior position but had markedly different dorsoventral positions, unambiguously demonstrating a failure to establish correct map topography along both axes (Figure 2B). Obvious dorsoventral abnormalities were seen both for temporal axons

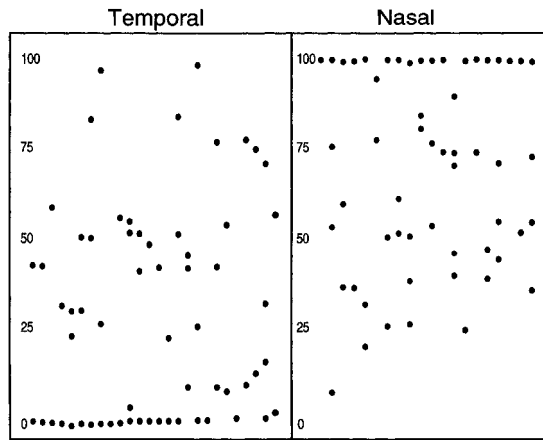


Figure 3. Summary of Topographic Map Defects in *ephrin-A2*^{-/-}; *ephrin-A5*^{-/-} Double Mutant Mice

Arborizations from 26 temporal and 20 nasal injections in *ephrin-A2*^{-/-}; *ephrin-A5*^{-/-} mutant mice were plotted with respect to a region along the anteroposterior axis. Zero represents the anterior end of the SC, and 100 the posterior end. Each black dot represents a distinct arborization site. Each vertically aligned set of dots represents a single retinal labeling.

(27% penetrance, 4/15 mice) and for nasal axons (53% penetrance, 8/15 mice). Arborizations were scattered over up to half of the dorsoventral axis of the SC in individual animals and did not appear to be targeted to any specific ectopic location or pattern.

To test whether retinal axons fill the SC, despite the severe topographic abnormalities, we injected fluoresceinated cholera toxin β subunit into the eye to anterogradely label ganglion cells throughout the retina. The results show that in double homozygotes retinal axons still fill the entire SC (Figures 2E and 2F).

Expression of Ephrins and Eph Receptors in Wild-Type and Mutant Mice

To help in understanding the mutant phenotypes, we examined the expression patterns of ephrin-A2 and ephrin-A5 in the midbrain, initially in wild-type mice. The results are broadly consistent with previous reports in mice (Cheng and Flanagan, 1994; Donoghue et al., 1996; Flenniken et al., 1996; Marcus et al., 1996; Zhang et al., 1996; Frisén et al., 1998). Ephrin-A2 RNA has a high point of expression at or just anterior to the SC/IC boundary, diminishing both toward the anterior end of the SC, and posteriorly into the IC (Figure 4A). The low point of expression appears to extend somewhat further in both anterior and posterior directions than in some previous studies, presumably reflecting a slightly greater sensitivity of detection. Ephrin-A5 RNA is expressed at the highest levels in the posterior IC, diminishing to low levels in the anterior SC (Figure 4B). The expression of ephrin-A5 RNA was not detectably affected in the *ephrin-A2*^{-/-} mutant, nor was ephrin-A2 RNA expression affected in the *ephrin-A5*^{-/-} mutant (data not shown; Frisén et al., 1998).

To test ligand distribution at the protein level, we used fusion protein probes consisting of Eph receptors fused to an alkaline phosphatase (AP) tag. Similar results were

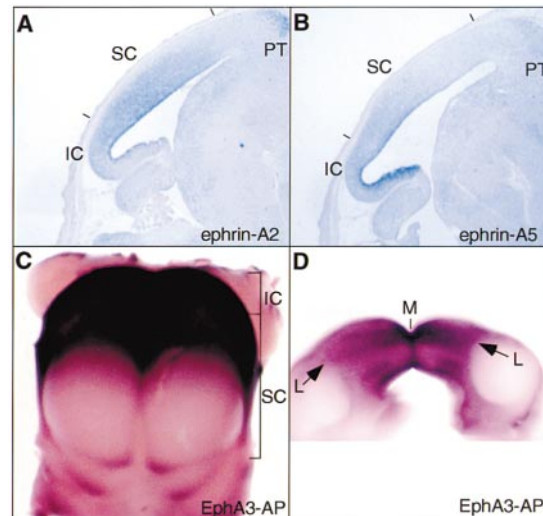


Figure 4. Ephrin-A2 and Ephrin-A5 Expression in Developing Mid-brain

(A and B) RNA hybridization on parasagittal E18 mouse brain sections. Lines indicate approximate anterior and posterior ends of the developing SC.

(A) Ephrin-A2 probe shows a high point of expression near or just anterior to the SC/IC boundary, decreasing in both anterior and posterior directions.

(B) Ephrin-A5 probe shows staining most prominently in the ventricular zone, with a high point in the posterior IC, decreasing anteriorly. (C and D) Detection of ligands by affinity probe in situ with an EphA3-AP fusion protein probe.

(C) Whole-mount E18 mouse brain, showing ligand expression in developing midbrain, highest in the IC and decreasing anteriorly.

(D) Coronal section of an E18 posterior SC showing differential staining in the mediolateral axis of the SC, with highest expression medially.

Abbreviations: SC, superior colliculus; IC, inferior colliculus; PT, pretectal nuclei; M, medial; L, lateral.

obtained with an EphA3-AP probe (Figure 4C) or an EphA5-AP probe (data not shown). A single gradient was seen across the midbrain, with strongest staining in the posterior IC, diminishing toward the anterior SC (Figure 4C). This overall gradient appears consistent with the ephrin-A2 and -A5 RNA patterns (Figures 4A and 4B) and supports the idea that these two ephrins form a single composite binding gradient across the midbrain. While the major asymmetry in this distribution is along the anteroposterior axis, there was also some indication of a differential distribution across the mediolateral axis of the SC (which corresponds to the dorsoventral mapping axis of the retina). In particular, in multiple experiments each lobe of the SC stained most strongly in medial areas while central areas stained less strongly, as seen in whole mounts and particularly in coronal sections (Figures 4C and 4D). However, this dorsoventral component is not nearly as prominent as the anteroposterior component.

We next wanted to test whether additional A ephrins might be present in the SC. We did this in two ways. First, in situ RNA hybridization was performed for all the other known ephrin-A family members, ephrin-A1, -A3, and -A4. We were unable to detect prominent expression of any of these in the SC or IC, consistent with

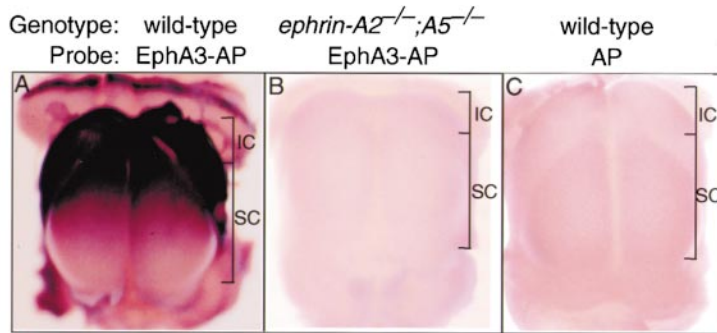


Figure 5. Loss of Binding Activity in *ephrin-A2^{-/-}; ephrin-A5^{-/-}* Mice

Wild-type P0 mice (A) show a gradient in ligand protein expression as detected by binding of an EphA3-AP fusion protein probe. Staining in the *ephrin-A2^{-/-}; ephrin-A5^{-/-}* double mutant (B) is greatly reduced, resembling background levels (C).

previous reports (data not shown; Flenniken et al., 1996; Zhang et al., 1996). Second, we performed receptor-AP binding experiments using EphA3-AP or EphA5-AP fusion protein probes to test *ephrin-A2^{-/-}; ephrin-A5^{-/-}* midbrains. In multiple experiments, we were unable to detect binding above background levels (Figure 5). It is not likely that ligand expression in posterior SC is strongly masked by high Eph receptor expression, since ligand-AP probing reveals little or no receptor in this region (data not shown). While the presence of unknown ligands cannot be eliminated, these results indicate that the greatest part, and perhaps all, of the SC gradient of ligands that interact with EphA receptors is made up of ephrin-A2 and -A5.

Receptor-AP staining also showed that ligands are expressed in the retina (Figure 6D), most prominently near the nasal end, consistent with previous reports in chick and mouse (Marcus et al., 1996; Connor et al., 1998; Hornberger et al., 1999). Like the ligand gradient in the SC, the prominent ligand expression in nasal retina was not detectable in the *ephrin-A2^{-/-}; ephrin-A5^{-/-}* double mutant (Figure 6H). We also tested retinal receptor protein expression using an ephrin-A5-AP probe, which revealed a temporal > nasal gradient (Figure 6C). Staining is seen throughout the thickness of the retina, consistent with the RNA expression for EphA5 and EphA6 in the ganglion cell layer (Figures 6A and 6B), as well as additional Eph receptors in outer retinal layers (Feldheim et al., 1998).

In principle, mapping abnormalities could be explained by a role for ephrins in establishing tangential pattern of the retina or SC, rather than a direct role in axon guidance. To address this, we tested the *ephrin-A2^{-/-}; ephrin-A5^{-/-}* double mutants for expression of regional markers. EphA5 is known to be in a temporal > nasal gradient across the mouse retina (Figure 6A; Feldheim et al., 1998). We find here that EphA6 is in a similar temporal > nasal gradient (Figure 6B). The receptor gradients were still present in the double mutants (Figures 6E, 6F, and 6G). In the mouse SC, EphA7 receptor RNA is expressed in an anterior > posterior gradient, and this gradient was also still present in the double mutant (data not shown). While the possibility of a subtle patterning difference cannot be eliminated, there did not appear to be any major change in the graded patterning of cell fates in the retina and tectum that could account for the mapping phenotype in the *ephrin-A2^{-/-}; ephrin-A5^{-/-}* mutant.

In Vitro Assays Show Ephrin-A2 and Ephrin-A5 Are Required for the Repellent Activity in Posterior SC and Also Modulate Retinal Axon Responsiveness

Tests for mapping abnormalities in the mutant mice do not resolve whether ephrin-A2 and ephrin-A5 act in the SC, the retina, or both. To examine this, we performed in vitro stripe assays in a mix-and-match format, where either the retinal explants or the SC membranes were taken from wild-type or mutant mice.

In the first series of experiments, we tested whether ephrin-A2 and ephrin-A5 are responsible for the topographically specific repellent activity in the SC. It has previously been shown in chick (Walter et al., 1987), mouse (Godement and Bonhoeffer, 1989), and rat (Roskies and O'Leary, 1994) that membranes from posterior tectum/SC will repel retinal axons or inhibit their branching in a topographically specific manner. Membranes from the IC of *ephrin-A5^{-/-}* mice have been shown to have a reduced outgrowth-inhibiting activity on retinal axons (Frisén et al., 1998). However, the effect of gene disruption has not previously been tested on topographically specific repulsion by SC membranes. To do this, we performed stripe assays with wild-type retinal axons growing on membranes from wild-type or mutant SC. Wild-type mouse posterior SC membranes repelled retinal axons, with a stronger effect on temporal axons (Figures 7A, 7C, and 7E) as reported previously (Godement and Bonhoeffer, 1989). However, when the SC membranes were derived from double mutant animals, the axons showed no detectable preference (Figures 7B and 7E).

To test by genetic loss-of-function whether ephrin-A2 and ephrin-A5 have a role in the retina, we compared wild-type and mutant retinal explants. Temporal axons from wild-type or *ephrin-A2^{-/-}; ephrin-A5^{-/-}* animals show avoidance of posterior membranes, with no significant effect of the mutation on sensitivity (Figure 7E). However, the mutation had a pronounced effect on nasal axons, which showed a much stronger preference for anterior SC lanes than wild-type nasal axons did ($p < 0.0002$, Wilcoxon rank sum test; Figure 7E). However, the responsiveness of mutant nasal axons remained weaker than the responsiveness of temporal axons ($p < 0.0005$; Figure 7E).

Discussion

The projection from the retina to the tectum, or its mammalian equivalent the SC, has long been a major model

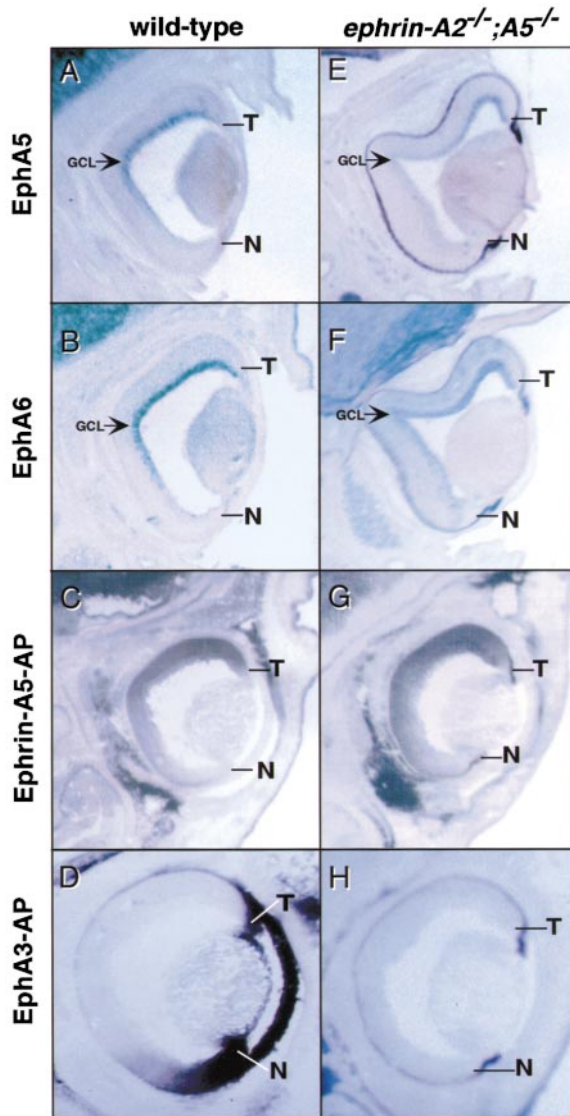


Figure 6. EphA Receptor Expression and Binding Patterns in Wild-Type and *ephrin-A2^{-/-}; ephrin-A5^{-/-}* Mice

Horizontal sections through the P0 eye from wild-type (A–D) or *ephrin-A2^{-/-}; ephrin-A5^{-/-}* (E–H) mice.

(A and B) EphA5 and EphA6 receptor RNAs are in the ganglion cell layer in a temporal > nasal gradient.

(C) Receptor protein detected with an ephrin-A5-AP probe is also in a temporal > nasal gradient.

(E–G) These receptor gradients remain in the double mutant.

(D) Ligand expression detected by binding of an EphA3-AP probe is highest in nasal retina.

(H) The double mutants show a loss of these binding sites.

Abbreviations: N, nasal; T, temporal; GCL, ganglion cell layer.

system to understand the development of topographic maps. Analysis of this projection therefore provides an opportunity to understand the basic mechanisms of mapping, both because of recent work at the molecular level and because of a history of outstanding experimental and theoretical analyses over a period of decades.

Two A ephrins, ephrin-A2 and -A5, are known to be expressed in the SC. An earlier analysis of the retinocollicular projection in *ephrin-A5^{-/-}* single mutant mice

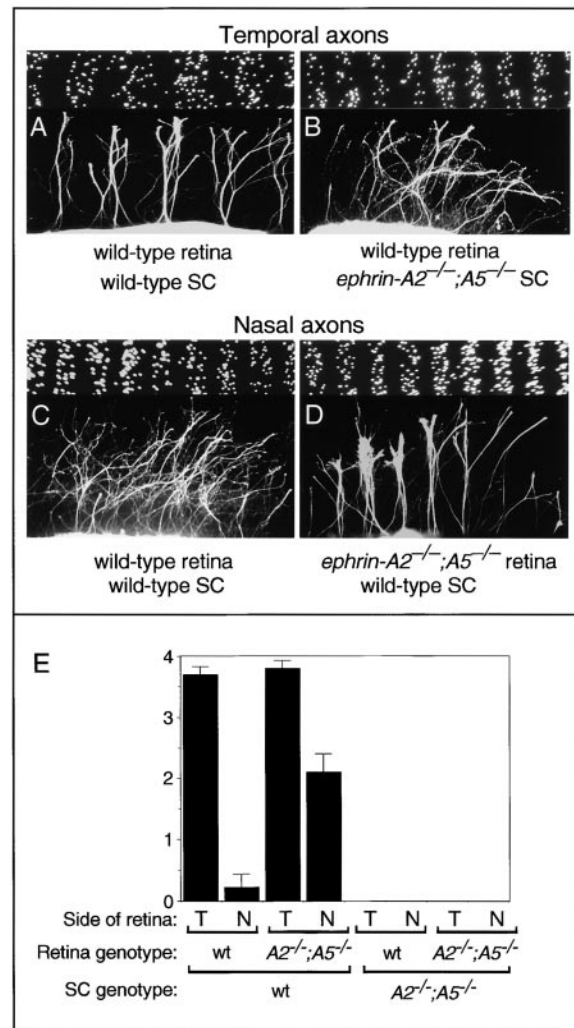


Figure 7. Mix-and-Match Stripe Assays Show Defects in Both the SC and the Retina of *ephrin-A2^{-/-}; ephrin-A5^{-/-}* Double Mutants

(A and B) Loss of repellent activity from posterior SC of mutant mice. Temporal axons from wild-type mice were tested with alternating anterior and posterior stripes of SC membranes from wild-type (A) or *ephrin-A2^{-/-}; ephrin-A5^{-/-}* mutant (B) mice.

(C and D) Gain in responsiveness of nasal axons from mutant mice. Nasal axons from wild-type (C) or *ephrin-A2^{-/-}; ephrin-A5^{-/-}* mutant (D) mice were grown on alternating anterior and posterior SC stripes from wild-type mice.

(E) Results of mix-and-match stripe assays using retina or SC from wild-type or *ephrin-A2^{-/-}; ephrin-A5^{-/-}* mice. Axon preference for anterior SC lanes was scored on a scale of 0 (no preference) to 4 (strong preference). Bars show means \pm SEM. Numbers of independent assays scored were: wild-type retina and SC, T = 14, N = 10; mutant retina plus wild-type SC, T = 10, N = 14; wild-type retina plus mutant SC, T = 15, N = 9; mutant retina and SC, T = 5, N = 4. Abbreviations: T, temporal; N, nasal.

showed moderate mapping errors, with temporal axons terminating in abnormally posterior positions. It was also shown that IC membranes lose in vitro outgrowth-inhibiting activity (Frisén et al., 1998). Here, we describe a study of the projection patterns of both temporal and nasal axons, in both ephrin-A2 and ephrin-A5 mutants, as well as double homozygote and double heterozygote combinations. This analysis uses a combination of

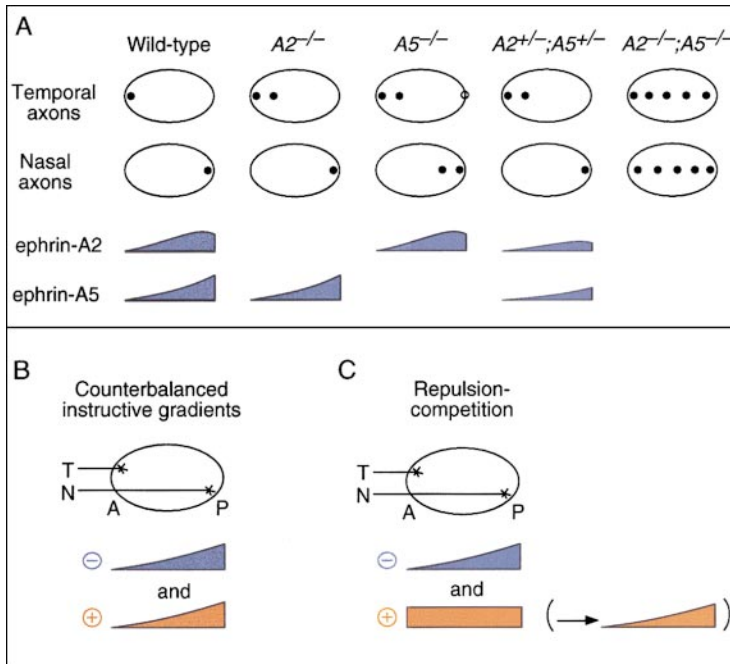


Figure 8. Models for the Action of Topographic Mapping Labels

(A) Schematic illustration of retinocollicular mapping phenotypes in mice with disrupted *ephrin-A2* or *ephrin-A5* genes. The SC is indicated as an oval, with anterior to the left. Closed circles illustrate regions where terminal arborizations are found. An open circle for the *ephrin-A5*^{-/-} mutant indicates a location at the SC/IC boundary where axons accumulate though do not appear as a usual tight arborization. Expression patterns of ephrin-A2 and -A5 are schematically illustrated below.

(B and C) Two alternative models for topographic map specification. In the retinocollicular system, temporal axons (T) terminate in anterior SC (A) and nasal axons (N) in posterior SC (P).

(B) Counterbalanced gradients are prespecified by mechanisms intrinsic to the target and create opposing forces on the axons. Axons from different retinal positions have differential sensitivity to one or both gradients, and each axon forms a termination zone at the position where the opposing forces cancel out. Repellent and attractant gradients are illustrated, though there are other possibilities such as oppositely oriented repellent gradients, or a single gradient with attractant or repellent effects at different concentrations.

(C) Repulsion/competition model. Axons compete with one another for space in the target. A gradient of repellent biases this competition: temporal axons are more sensitive to the repellent, so they terminate in anterior SC, while nasal axons are less sensitive and can terminate in posterior SC. Nasal axons do not terminate in the anterior SC because of greater competition there. The model is illustrated as a competition for positive permissive factors in the SC, though axon-axon repulsion could also contribute. In this model the graded negative factor is topographically specific. The initial expression of the positive factor could be somewhat graded, but it could be broadly expressed through the target and could be entirely permissive as illustrated here. While the mechanism of competition is currently unknown, we suggest as an optional extension of the model that competition for the permissive factor may be greatest in the anterior SC and, as illustrated in brackets, this could create a secondary, induced gradient in availability of the positive factor.

vivo axon tracing, as well as in vitro assays of topographically specific activities in the SC and responses in the retina. Below, we discuss the implications of our findings for the basic mechanisms of topographic mapping.

Specification of Topographic Position: Gradient and Competition Models

Previous characterizations of in vitro activities and expression patterns have suggested that ephrin-A2 and -A5 act in retinotectal/retinocollicular mapping as repellents: they repel temporal axons in vitro and when over-expressed in vivo, and are expressed in the target in countergradients with respect to retinal EphA receptors. Therefore, considering that they are expressed in posterior > anterior gradients, a simple prediction for the removal of these ephrins would be that termination sites of retinal axons should tend to shift in a posterior direction. Indeed, in *ephrin-A5*^{-/-} mice (Frísén et al., 1998) as well as *ephrin-A2*^{-/-} mice, double heterozygotes, and double homozygotes, axons labeled near the temporal extreme of the retina do arborize in abnormally posterior regions (Figure 8A), consistent with a loss of repellent activity from the posterior SC (or loss of an activity that inhibits branching or arborization, which will be treated here as formally equivalent.)

However, this simple model of a loss of repellents does not by itself account for the behavior of nasal axons (Figure 8A). We find that rather than shifting posteriorly,

axons labeled near the nasal extreme of the retina show an anterior shift in the SC of *ephrin-A5*^{-/-} mice, and this effect is even greater in *ephrin-A2*^{-/-}; *ephrin-A5*^{-/-} double mutants. How can this be explained?

One model that could help account for the nasal axon phenotype is based on a loss of ephrin function in the retina. We find here that nasal axons from ephrin mutant mice become more responsive to ephrins in vitro, as discussed further below. This gain in sensitivity could cause nasal axons to respond to lower levels of ephrins in the target and therefore to map in abnormally anterior positions. In *ephrin-A5*^{-/-} single mutants, where the axons can respond to ephrin-A2 in the target, this model might help explain the direction of shift of nasal axons in both the SC (this study) and the lateral geniculate nucleus (LGN) (Feldheim et al., 1998). However, this model does not easily explain the double mutant phenotype. In the SC of *ephrin-A2*^{-/-}; *ephrin-A5*^{-/-} mice, we could not detect ephrin expression with EphA receptor fusion probes. Moreover, we could detect no in vitro repellent activity when double mutant SC membranes were tested on retinal axons from either wild-type or mutant mice. Despite this, the nasal axons map even more anteriorly in the double mutant than in the *ephrin-A5*^{-/-} single mutant. Therefore, it does not seem likely that the stop-short phenotype of axons in the double mutant is due solely to an increased response to repellent ephrins in the target.

It is interesting to consider these results in the light of theoretical models that have been proposed for topographic map specification. Currently, a leading model is that both attractant and repellent gradients may be prespecified within the target (Figure 8B; Gierer, 1981; O'Leary et al., 1999). Each axon then identifies its correct termination zone as the point where repellent and attractant forces cancel out. In this model, wild-type nasal axons map to posterior SC because they are attracted there. A prediction of this model is that in the *ephrin-A2^{-/-}; ephrin-A5^{-/-}* double mutant, axons would tend to map more posteriorly than normal, or in the case of extreme nasal axons might show no shift. This appears to be contrary to our results, especially considering that the opposite shifts in the nasal and temporal axons are of similar magnitudes. For similar reasons our results do not seem consistent with a variant of the counterbalanced gradient model, where a posterior > anterior ephrin gradient would be balanced by a prespecified repellent in an anterior > posterior gradient. An alternative possibility that could perhaps be reconciled with our results would be for ephrins in the target to act as either repellents or attractants at different concentrations (Gierer, 1981; Honda, 1998), although there is currently no direct evidence to support such an effect from axon guidance assays.

As an alternative to models with two counterbalanced gradients prespecified in the target, we propose that our results could be explained by a model involving a repellent gradient of ephrins, in combination with axon-axon competition (Figure 8C). This competition could be for limiting positive factors in the target (Figure 8C) or could also involve direct axon-axon interactions. We previously suggested a model of this type in our analysis of the LGN in *ephrin-A5^{-/-}* mice (Feldheim et al., 1998), and the model now receives strong support from our more comprehensive analysis in the SC. The repulsion/competition model would account for normal mapping as follows. Temporal axons would be unable to terminate in posterior SC, because they are repelled by the ephrins, so they would be forced to arborize in anterior SC. Nasal axons are less sensitive to ephrin repulsion and so would be able to terminate in posterior SC. In anterior SC, nasal axons face greater competition for limiting amounts of permissive factor(s), so they prefer to avoid this competition and arborize only in posterior SC.

Incorporating competition in the model can explain several aspects of our data. First, nasal axons shift anteriorly in the *ephrin-A5^{-/-}* single mutant (although this could be explained by the axon sensitivity model outlined above), and shift even further anteriorly in the *ephrin-A2^{-/-}; ephrin-A5^{-/-}* double mutant. According to the competition model, posterior repellents are removed, so axons from temporal or central retina are now able to compete more effectively in posterior SC; nasal axons therefore face increased competition in posterior SC, so they lose their strong preference for this region and spread out into more anterior regions. The model thus seems to fit well with the opposite and quantitatively similar shifts of axons from temporal and nasal extremes of the retina. Labelings at intermediate retinal positions are more difficult to characterize because of the lack of fixed landmarks but, consistent with

the competition model, such labelings revealed multiple arborizations, seemingly shifted in both anterior and posterior directions (data not shown). Second, axons are not respecified to a specific ectopic position. Instead, arborizations are scattered over an abnormally broad zone in the mutants, including both normal and abnormal regions. This is the result predicted by the competition model: as the topographically specific repellents are removed, axons would spread into abnormal regions, but there is no reason for them to disfavor the correct region. Third, even in the *ephrin-A2^{-/-}; ephrin-A5^{-/-}* mutant, we find that retinal axons fill the entire SC and that axons from both nasal and temporal extremes of the retina form connections within the target. Models that involve a strict matching of values in the projecting and target field would predict that the mutant should have unmatched areas, whereas the competition model predicts that the entire projecting and target fields should still match up.

Our repulsion/competition model also seems consistent with a large body of earlier work involving ablations of parts of the retina or tectum/SC in rodents (Finlay et al., 1979; Simon et al., 1994) and other species (Fraser and Hunt, 1980). Those experiments indicated that, at least under some experimental conditions, retinal axons tend to spread out and fill the available space in the target. Since molecular labels had not been identified when those studies were initially performed, two explanations could not be distinguished: either the labeling gradients readjust, or mapping may involve axon-axon competition. Indeed, several competition models for mapping have been proposed (Prestige and Willshaw, 1975; Fraser and Hunt, 1980) although the idea has received less attention in the last decade (see Goodhill and Richards, 1999). In molecular terms, candidates for limiting permissive factors that might be responsible for axon-axon competition in the tectum/SC include adhesion molecules, growth factors, or neurotrophic factors such as BDNF (Fraser and Hunt, 1980; Cohen-Cory and Fraser, 1995; McFarlane et al., 1996; Inoue and Sanes, 1997), although *BDNF* knockout mice are capable of forming a retinocollicular map (unpublished data).

In the competition model proposed here (Figure 8C) the negative factors have an instructive role as prespecified topographic labels. While we cannot rule out some prespecified gradation in the positive factors too, they could be produced broadly through the target and could have an entirely permissive role. However, we would predict that during part or all of the mapping period, competition for positive factors may be greatest in the anterior SC—due to a higher density of axonal structures or their entry at the anterior end—and that processes such as masking or internalization may produce a secondary, induced gradient in availability of the positive factors (Figure 8C). This is in contrast to the idea of an attractant gradient fully prespecified by patterning mechanisms intrinsic to the target (Gierer, 1981; O'Leary et al., 1999). However, the molecular mechanism we suggest may be very consistent with a mathematical model proposed by Gierer as a possible extension of his basic counterbalanced gradient scheme: "An extreme case . . . would be to assume . . . that only one of the gradients in the tectum is pre-existing; the other . . . is newly produced on the tectum upon innervation"

(Gierer, 1983). The idea of an attractant gradient induced by competition could bring some unification to the idea of counterbalanced gradients and competition, which have often been viewed as distinct or even contradictory mechanisms.

In addition to their ability to explain available experimental data, competition models could have an important biological advantage. During development or evolution, if there are slight variations in the concentrations of the graded labeling molecules, axon-axon competition will tend to ensure that the axons will always spread out to fill the entire target. This mechanism can therefore ensure the formation of a robust map with a match of connections between projecting and target areas.

Multiple Termination Zones and Map Refinement

One of the notable features of the ephrin mutants studied here is that following focal Dil labeling in the retina, the termination zones always took the form of punctate spots in the SC. In the double mutant, relative to the single mutants, the spots became more numerous and more scattered, but each remained as a tight focus. How can this be explained?

In the *ephrin-A2*^{-/-} and *ephrin-A5*^{-/-} single mutants, a major spot was always seen at or near the topographically appropriate position (this study; Frisén et al., 1998). This could potentially be consistent with two populations of retinal ganglion cells, one dependent on ephrins for mapping and the other independent. In the double mutant, however, the spot found at or near the normal position was of variable intensity, and was sometimes weak or absent. This makes the two-population model seem unlikely.

An alternative model for the punctate termination zones could involve a mechanism that causes neighboring axons in the retina to cluster together in the SC, such as Hebbian activity-dependent refinement. The basic idea is that axons which fire at similar times, because of patterned vision or spontaneous retinal waves, would have their connections reinforced if they are clustered in the target (Shatz, 1996). In the ephrin mutants, we suggest that removal of activity-independent labels may allow axons from a small retinal position to terminate over an abnormally broad region of the SC. Activity-dependent mechanisms may cluster the connections but may act over only a limited distance, so rather than a single cluster they form several arbitrary foci scattered within the overall region. This model could explain why the average number of termination zones in the different types of mutant tends to increase in parallel with the area over which they are scattered.

Do Axons Detect Absolute or Relative Ephrin Levels?

A basic question about the mapping mechanism is whether axons respond to absolute or relative levels of labeling molecules. This has previously been addressed by in vitro studies, where the critical factor was concluded to be either gradient steepness (Baier and Bonhoeffer, 1992) or the increase in concentration relative to the starting level (Rosentreter et al., 1998). Our analysis, particularly of the *ephrin-A2*^{+/-}; *ephrin-A5*^{+/-} double

heterozygote, provides an alternative way to address this question.

At one extreme one might suppose only the shape of the gradient matters, and the absolute value makes no difference. However, our results do not support this model, since the *ephrin-A2*^{+/-}; *ephrin-A5*^{+/-} double heterozygotes do have a phenotype. At the other extreme, axons might be preprogrammed to recognize only a specific level of ephrin in the target. However, our results do not support this model either, since there was no nasal axon phenotype in the *ephrin-A2*^{+/-}; *ephrin-A5*^{+/-} mutant. Our results seem consistent with an alternative model based on mapping precision. The ability of axons to discriminate between any two points on the tectum would depend on those two points having a sufficiently great difference in ephrin concentration. If the difference in concentration between nearby points is reduced, mapping precision will be reduced and the axons will tend to spread out over a wider region. This model may be compatible with the in vitro results obtained previously (Baier and Bonhoeffer, 1992; Rosentreter et al., 1998) and seems consistent with the abnormalities of temporal and nasal axons seen in all the genotypes examined here (Figure 8A).

Overlapping Gradients: Additive and Distinct Functions of Ephrin-A2 and -A5

One of the notable characteristics of the ephrin family is that in many parts of the embryo two or more ligands are expressed in overlapping gradients. Our studies permit an in vivo analysis of the significance of this overlap.

First, our finding that the double homozygous mutant shows a synergistic phenotype more severe than either single mutant demonstrates that ephrin-A2 and ephrin-A5 are partially redundant in topographic mapping.

A further question is to what degree they have distinct roles. Based on the *ephrin-A5*^{-/-} analysis, it was previously suggested that ephrin-A5 might have a dominant role in both anterior and posterior SC, whereas ephrin-A2 may act in central regions (Frisén et al., 1998). Confirming the idea that ephrin-A5 is dominant in posterior tectum, we find here that nasal axon mapping is normal in the *ephrin-A2*^{-/-} mutant. This posterior dominance of ephrin-A5 seems to fit well with its steeper posterior gradient and with its higher affinity for Eph receptors (Drescher et al., 1997; Flanagan and Vanderhaeghen, 1998).

In contrast, the temporal axon phenotypes here provide evidence of an additive function of ephrins. In particular, strong support for this idea comes from the finding that *ephrin-A2*^{-/-}, *ephrin-A5*^{-/-}, and *ephrin-A2*^{+/-}; *ephrin-A5*^{+/-} mice all show a similar temporal axon phenotype in anterior SC (Figure 8A). Our study therefore provides in vivo functional evidence to support the idea, initially based on binding studies (Brambilla et al., 1996; Gale et al., 1996), that there may be a high degree of promiscuity and interchangeability in the functions of different ephrins.

Ephrins Act in Both the Retina and the Tectum

We show here by a genetic loss-of-function approach that ephrin-A2 and -A5 are required for normal responsiveness of retinal axons. Specifically, nasal axons in

the *ephrin-A2*^{-/-}; *ephrin-A5*^{-/-} mutant become more responsive than normal. These results fit well with studies in chick showing that retinal overexpression of ephrin-A5 causes axons to map more posteriorly in the tectum, and that treatment of the retina with PI-PLC (which removes ephrins of the A class as well as other GPI-anchored proteins) causes nasal axons to become more sensitive to ephrins (Hornberger et al., 1999). All these findings seem consistent with a model where ephrins in nasal retina may act to mask or downregulate Eph receptors. Nevertheless, nasal axons taken from the *ephrin-A2*^{-/-}; *ephrin-A5*^{-/-} mutant remain less responsive than temporal axons, consistent with the idea that Eph receptor gradients can also by themselves determine retinal sensitivity (Cheng et al., 1995). The countergradients of ligand and receptor within the retina may generate a steeper gradient of functional receptors and thereby increase the precision of mapping.

Are There Additional Anteroposterior Labels?

In the *ephrin-A2*^{-/-}; *ephrin-A5*^{-/-} double mutant, both nasal and temporal axons can arborize in any anteroposterior region. These two ephrins are therefore essential for orderly topographic mapping throughout the SC. However, some degree of topographic bias remains in the double mutant. Several explanations of this are possible. There might be low levels of an additional A ephrin that was not detected here. B ephrins might contribute to anteroposterior mapping. Also, molecules in other families might act as topographically specific attractants or repellents (see, e.g., Muller et al., 1996). In this regard, we should note that although our results do not seem consistent with mapping exclusively by prespecified counterbalanced gradients, this does not rule out the presence of additional gradients. It is also possible that some degree of topographic order could be established in the absence of labels, for example by mechanisms based on the timing of axon outgrowth and arrival.

Dorsoventral Mapping Errors in *ephrin-A2*^{-/-}; *ephrin-A5*^{-/-} Double Mutants

The molecular basis of dorsoventral mapping is not well understood. Recent studies have identified zebrafish mutations that affect dorsoventral mapping (Trowe et al., 1996) and have identified nuclear factors implicated in setting up dorsoventral pattern in the retina (Schulte et al., 1999). One of the unexpected findings from our mutant analysis here is that although ephrin-A2 and -A5 had previously been implicated only in anteroposterior guidance, the *ephrin-A2*^{-/-}; *ephrin-A5*^{-/-} mice show prominent dorsoventral abnormalities. These results provide the first demonstration of ephrins that are required for mapping this axis.

Our results lead to two possible models: either the dorsoventral mapping phenotype is a primary effect of the loss of dorsoventral labels, or it is a secondary effect of the loss of anteroposterior labels. Our analysis here cannot distinguish conclusively between these possibilities. If ephrins were acting directly as dorsoventral labels, they should be expressed differentially across this axis. Supporting this, we do find that there are differences in ephrin expression across the dorsoventral/mediolateral axis of the SC, although the differences are

much more subtle than the prominent anteroposterior gradients. One might also expect, if A ephrins are dorsoventral labels, that this should be detectable by in vitro axon guidance assays. Such assays have so far failed to provide evidence for dorsoventral labels (Walter et al., 1987; data not shown). However, it is possible that the available in vitro assays may not reliably detect subtle differences that might nevertheless have a significant effect in vivo.

The alternative idea that the dorsoventral defect in the mutants may be secondary to the anteroposterior defect may be plausible, especially considering the time course of mapping during development. With respect to the anteroposterior axis, mouse retinal axons enter the SC at its anterior end, initially overshoot, and subsequently form collateral branches at their topographically correct position and retract the overshooting segment (Simon and O'Leary, 1992). Along the dorsoventral axis, some differences between nasal and temporal axons are already apparent as axons enter the tectum, but final dorsoventral topography is achieved by side branching after anteroposterior position is determined (Simon and O'Leary, 1992). It is therefore possible that establishing anteroposterior topography is an obligate first step before final dorsoventral corrections are made. If so, in the *ephrin-A2*^{-/-}; *ephrin-A5*^{-/-} double mutant, an inability of axons to identify a specific anteroposterior position may result in a failure to activate the machinery required to read dorsoventral cues. This model would indicate that further studies of the timing of these events and the degree to which they may be linked in vivo or in vitro may help in unraveling the poorly understood role of labels in dorsoventral mapping, and in understanding how a full two-dimensional map is formed.

Conclusion

We report here a genetic study involving disruption of both A ephrins known to be expressed in the retinotectal projection. The results provide a test of models for retinotectal map specification that have been proposed over the last 50 years, supporting a repulsion/competition model of label-guided mapping. These studies also provide genetic evidence for aspects of mapping not anticipated in the traditional models, including a requirement for ephrin-A2 and -A5 in both retina and target and a requirement for these ephrins in specification of both axes of the two-dimensional map. Finally, the results provide a genetic test of the significance of overlapping ephrin gradients, providing in vivo functional evidence that ephrins can have distinctive actions and can also act in an additive fashion. Ephrins appear to act as labels in many, and possibly all, topographic maps of connections between neurons (Flanagan and Vanderhaeghen, 1998), as well as connections between neurons and muscles (Feng et al., 2000). The basic principles of ephrin action in the retinocollicular projection are therefore likely to be broadly applicable to the development of neural maps.

Experimental Procedures

Gene Targeting

To make a targeting construct, ephrin-A2 cDNA (Cheng and Flanagan, 1994) was used to screen a strain 129SvEv lambda genomic

library (a kind gift of Dr. P. Leder). A targeting construct, pPNT-ELF1, was made using vector pPNT (Tybulewicz et al., 1991), with a 4.5 kb EcoRV-EcoRV fragment upstream and a 5 kb EcoRV-EcoRI fragment downstream of the neomycin cassette, and an insertion site after base pair 198 of the ephrin-A2 protein coding region. XbaI-linearized pPNT-ELF1 was electroporated into the EC cell line TC1 as described (Deng et al., 1994). Colony genomic DNA was analyzed by cutting with XbaI, followed by Southern analysis with a probe 3' to the EcoRV-EcoRI arm of the targeting construct. Evaluation of 114 independent clones revealed 14 that had been correctly targeted. Cells from two independent clones were microinjected into blastocysts, and germline transmission of the mutated *ephrin-A2* allele was monitored by Southern blotting. Routine genotyping was by PCR of tail genomic DNA, using primers *ggctataccgtggaggtg* and *ctgccggtggcacagga* for the wild-type *ephrin-A2* locus and the *neo* primer *ccgcttctctgtcttaccggtatc*. The wild-type allele generates a 110 bp amplified product and the mutant allele a 575 bp product. To confirm disruption at the RNA level, the same primers were used to amplify cDNA derived from E17 midbrain, showing a 110 bp amplified product from wild-type and *ephrin-A2*^{+/-} mice that was absent from *ephrin-A2*^{-/-} mice. PCR analysis of the ephrin-A5 locus was as described (Frisén et al., 1998).

In Situ Analysis

Hybridization probes for mouse ephrin-A2 (Cheng and Flanagan, 1994), ephrin-A5, EphA5 (Feldheim et al., 1998), and EphA6 (Maisonnier et al., 1993) were used for in situ hybridization as described (Feldheim et al., 1998). Affinity probe in situ using EphA3-AP, EphA4-AP, EphA5-AP, and ephrin-A5-AP fusion proteins was also performed as described (Feldheim et al., 1998).

Axon Tracing

The eyelid was cut open, and 0.1–1 µl of 10% Dil in dimethyl formamide was injected at the temporal or nasal extreme of the retina with a fine glass micropipette using a Picospritzer II (General Valve). One to two days later, at P12–P20, mice were analyzed blind to genotype. The age distributions of the wild-type and mutant groups was similar, and indistinguishable results were obtained throughout the age range. After fixation by cardiac perfusion with 4% paraformaldehyde in PBS, midbrains were photographed with fluorescence optics as whole mounts and then as 200 µm vibratome sections. Arborizations were confirmed by their appearance at high magnification. The SC boundaries were identified by their characteristic shape and location in visible light or autofluorescence. All injected retinas were photographed as flat mounts. Since there is no prominent optic fissure in mice, orientation was determined according to the initial injection site. There was no obvious difference in the size, location, or appearance of the labeling sites, or the size of the retinas, that could account for the differences in the mutant projections. Whole eye fills with fluoresceinated cholera toxin β subunit (List Biological, Campbell, CA) were performed by injecting 2–5 µl of a 0.2% solution in 2% DMSO into the vitreous of P12 mice and examining the SC 48 hr later as a whole mount.

In Vitro Stripe Assays

The membrane stripe assay (Walter et al., 1987) was used essentially as previously described for mouse (Feldheim et al., 1998). Membranes from P0 anterior or posterior SC were laid down as alternating lanes, with red fluorescent microspheres added to one preparation. Strips from temporal or nasal extremes of E16 retinas were cut parallel to the dorsoventral axis. After 36–48 hr, axons were labeled with fluorescent vital dye and photographed. Growth preference for each explant was scored on a 0–4 scale, where 0 was no bias for either set of lanes and 4 was a strong bias. Explants were scored only if lanes were distinct as indicated by the microsphere marking and outgrowth was sufficient to judge preference.

Acknowledgments

We thank David Simon, Michael Hansen, Philip Leder, Cathie Daugherty, Ann Harrington, Gerard Dallal, Miriam Osterfield, Masaru Nakamoto, Pierre Vanderhaeghen, Qiang Lu, and David Van Vactor for

help, advice, and discussions. This work was supported by a fellowship from the National Eye Institute (D. A. F.), a fellowship and scholarship from the Canadian Medical Research Council (Y. I. K.), support from the Swedish Medical Research Council (J. F.), and National Institutes of Health grants EY11559 and HD29417 (J. G. F.).

Received December 21, 1999; revised February 8, 2000.

References

- Baier, H., and Bonhoeffer, F. (1992). Axon guidance by gradients of a target-derived component. *Science* **255**, 472–475.
- Braisted, J.E., McLaughlin, T., Wang, H.U., Friedman, G.C., Anderson, D.J., and O'Leary, D.D.M. (1997). Graded and lamina-specific distributions of ligands of EphB receptor tyrosine kinases in the developing retinotectal system. *Dev. Biol.* **191**, 14–28.
- Brambilla, R., Bruckner, K., Orioli, D., Bergemann, A.D., Flanagan, J.G., and Klein, R. (1996). Similarities and differences in the way transmembrane-type ligands interact with the Elk subclass of Eph receptors. *Mol. Cell. Neurosci.* **8**, 199–209.
- Cerretti, D.P., and Nelson, N. (1998). Characterization of the genes for mouse LERK-3/Ephrin-A3 (Epl3), mouse LERK-4/Ephrin-A4 (Epl4), and human LERK-6/Ephrin-A2 (EPLG6): conservation of intron/exon structure. *Genomics* **47**, 131–135.
- Cheng, H.-J., and Flanagan, J.G. (1994). Identification and cloning of ELF-1, a developmentally expressed ligand for the Mek4 and Sek receptor tyrosine kinases. *Cell* **79**, 157–168.
- Cheng, H.-J., Nakamoto, M., Bergemann, A.D., and Flanagan, J.G. (1995). Complementary gradients in expression and binding of ELF-1 and Mek4 in development of the topographic retinotectal projection map. *Cell* **82**, 371–381.
- Cohen-Cory, S., and Fraser, S.E. (1995). Effects of brain-derived neurotrophic factor on optic axon branching and remodelling in vivo. *Nature* **378**, 192–196.
- Connor, R.J., Menzel, P., and Pasquale, E.B. (1998). Expression and tyrosine phosphorylation of Eph receptors suggest multiple mechanisms in patterning of the visual system. *Dev. Biol.* **193**, 21–35.
- Deng, C.X., Wynshaw-Boris, A., Shen, M.M., Daugherty, C., Ornitz, D.M., and Leder, P. (1994). Murine FGFR-1 is required for early postimplantation growth and axial organization. *Genes Dev.* **8**, 3045–3057.
- Donoghue, M.J., Lewis, R.M., Merlie, J.P., and Sanes, J.R. (1996). The Eph kinase ligand AL-1 is expressed by rostral muscles and inhibits outgrowth from caudal neurons. *Mol. Cell. Neurosci.* **8**, 185–198.
- Drescher, U., Kremoser, C., Handwerker, C., Löscherer, J., Noda, M., and Bonhoeffer, F. (1995). In vitro guidance of retinal ganglion cell axons by RAGS, a 25 kDa tectal protein related to ligands for Eph receptor tyrosine kinases. *Cell* **82**, 359–370.
- Drescher, U., Bonhoeffer, F., and Müller, B. (1997). The Eph family in retinal axon guidance. *Curr. Opin. Neurobiol.* **7**, 75–80.
- Feldheim, D.A., Vanderhaeghen, P., Hansen, M.J., Frisen, J., Lu, Q., Barbacid, M., and Flanagan, J.G. (1998). Topographic guidance labels in a sensory projection to the forebrain. *Neuron* **21**, 1303–1313.
- Feng, G., Laskowski, M.B., Feldheim, D.A., Wang, H., Lewis, R., Frisen, J., Flanagan, J.G., and Sanes, J.R. (2000). Roles for ephrins in positionally selective synaptogenesis between motor neurons and muscle fibers. *Neuron* **25**, 295–306.
- Finlay, B.L., Schneps, S.E., and Schneider, G.E. (1979). Orderly compression of the retinotectal projection following partial tectal ablation in the newborn hamster. *Nature* **280**, 153–155.
- Flanagan, J.G., and Vanderhaeghen, P. (1998). The ephrins and Eph receptors in neural development. *Annu. Rev. Neurosci.* **21**, 309–345.
- Flenniken, A.M., Gale, N.W., Yancopoulos, G.D., and Wilkinson, D.G. (1996). Distinct and overlapping expression patterns of ligands for Eph-related receptor tyrosine kinases during mouse embryogenesis. *Dev. Biol.* **179**, 382–401.
- Fraser, S.E., and Hunt, R.K. (1980). Retinotectal specificity: models

- and experiments in search of a mapping function. *Annu. Rev. Neurosci.* 3, 319–352.
- Frisen, J., Yates, P.A., McLaughlin, T., Friedman, G.C., O'Leary, D.D.M., and Barbacid, M. (1998). Ephrin-A5 (AL-1/RAGS) is essential for proper retinal axon guidance and topographic mapping in the mammalian visual system. *Neuron* 20, 235–243.
- Gale, N.W., Holland, S.J., Valenzuela, D.M., Flenniken, A., Pan, L., Ryan, T.E., Henkemeyer, M., Strebhardt, K., Hirai, H., Wilkinson, D.G., et al. (1996). Eph receptors and ligands comprise two major specificity subclasses and are reciprocally compartmentalized during embryogenesis. *Neuron* 17, 9–19.
- Gierer, A. (1981). Development of projections between areas of the nervous system. *Biol. Cybern.* 42, 69–78.
- Gierer, A. (1983). Model for the retino-tectal projection. *Proc. R. Soc. Lond. B Biol. Sci.* 218, 77–93.
- Godement, P., and Bonhoeffer, F. (1989). Cross-species recognition of tectal cues by retinal fibers in vitro. *Development* 106, 313–320.
- Goodhill, G.J., and Richards, L.J. (1999). Retinotectal maps: molecules, models and misplaced data. *Trends Neurosci.* 22, 529–534.
- Holash, J.A., and Pasquale, E.B. (1995). Polarized expression of the receptor protein tyrosine kinase Cdk5 in the developing avian visual system. *Dev. Biol.* 172, 683–693.
- Honda, H. (1998). Topographic mapping in the retinotectal projection by means of complementary ligand and receptor gradients: a computer simulation study. *J. Theor. Biol.* 192, 235–246.
- Hornberger, M.R., Dutting, D., Ciossek, T., Yamada, T., Handwerker, C., Lang, S., Weth, F., Huf, J., Wessel, R., Logan, C., et al. (1999). Modulation of EphA receptor function by coexpressed ephrinA ligands on retinal ganglion cell axons. *Neuron* 22, 731–742.
- Inoue, A., and Sanes, J.R. (1997). Lamina-specific connectivity in the brain: regulation by N-cadherin, neurotrophins, and glycoconjugates. *Science* 276, 1428–1431.
- Kenny, D., Bronner-Fraser, M., and Marcelle, C. (1995). The receptor tyrosine kinase Qek5 mRNA is expressed in a gradient within the neural retina and the tectum. *Dev. Biol.* 172, 708–716.
- Maisonpierre, P.C., Barrezaeta, N.X., and Yancopoulos, G.D. (1993). EHK-1 and EHK-2: two novel members of the Eph receptor-like tyrosine kinase family with distinctive structures and neuronal expression. *Oncogene* 8, 3277–3288.
- Marcus, R.C., Gale, N.W., Morrisson, M.E., Mason, C.A., and Yancopoulos, G.D. (1996). Eph family receptors and their ligands distribute in opposing gradients in the developing mouse retina. *Dev. Biol.* 180, 786–789.
- McFarlane, S., Cornel, E., Amaya, E., and Holt, C.E. (1996). Inhibition of FGF receptor activity in retinal ganglion cell axons causes errors in target recognition. *Neuron* 17, 245–254.
- Monschau, B., Kremoser, C., Ohta, K., Tanaka, H., Kaneko, T., Yamada, T., Handwerker, C., Hornberger, M.R., Loschinger, J., Pasquale, E.B., et al. (1997). Shared and distinct functions of RAGS and ELF-1 in guiding retinal axons. *EMBO J.* 16, 1258–1267.
- Muller, K., Jay, D., and Bonhoeffer, F. (1996). Chromophore-assisted laser inactivation of a repulsive axonal guidance molecule. *Curr. Biol.* 6, 1497–1502.
- Nakamoto, M., Cheng, H.-J., Friedman, G.C., McLaughlin, T., Hansen, M.J., Yoon, C., O'Leary, D.D.M., and Flanagan, J.G. (1996). Topographically specific effects of ELF-1 on retinal axon guidance in vitro and retinal axon mapping in vivo. *Cell* 86, 755–766.
- O'Leary, D.D., Yates, P.A., and McLaughlin, T. (1999). Molecular development of sensory maps: representing sights and smells in the brain. *Cell* 96, 255–269.
- Prestige, M.C., and Willshaw, D.J. (1975). On a role for competition in the formation of patterned neural connexions. *Proc. R. Soc. Lond. B Biol. Sci.* 190, 77–98.
- Rosentreter, S.M., Davenport, R.W., Loschinger, J., Huf, J., Jung, J., and Bonhoeffer, F. (1998). Response of retinal ganglion cell axons to striped linear gradients of repellent guidance molecules. *J. Neurobiol.* 37, 541–562.
- Roskies, A.L., and O'Leary, D.D.M. (1994). Control of topographic retinal axon branching by membrane-bound molecules. *Science* 265, 799–803.
- Schulte, D., Furukawa, T., Peters, M.A., Kozak, C.A., and Cepko, C.L. (1999). Misexpression of the Emx-related homeobox genes cVax and mVax2 ventralizes the retina and perturbs the retinotectal map. *Neuron* 24, 541–553.
- Shatz, C.J. (1996). Emergence of order in visual system development. *Proc. Natl. Acad. Sci. USA* 93, 602–608.
- Simon, D.K., and O'Leary, D.D.M. (1992). Development of topographic order in the mammalian retinocollicular projection. *J. Neurosci.* 12, 1212–1232.
- Simon, D.K., Roskies, A.L., and O'Leary, D.D.M. (1994). Plasticity in the development of topographic order in the mammalian retinocollicular projection. *Dev. Biol.* 162, 384–393.
- Sperry, R.W. (1963). Chemoaffinity in the orderly growth of nerve fiber patterns and connections. *Proc. Natl. Acad. Sci. USA* 50, 703–710.
- Trowe, T., Klostermann, S., Baier, H., Granato, M., Crawford, A.D., Grunewald, B., Hoffmann, H., Karlstrom, R.O., Meyer, S.U., Muller, B., et al. (1996). Mutations disrupting the ordering and topographic mapping of axons in the retinotectal projection of the zebrafish, *Danio rerio*. *Development* 123, 439–450.
- Tybulewicz, V.L., Crawford, C.E., Jackson, P.K., Bronson, R.T., and Mulligan, R.C. (1991). Neonatal lethality and lymphopenia in mice with a homozygous disruption of the c-abl proto-oncogene. *Cell* 65, 1153–1163.
- Walter, J., Henke-Fahle, S., and Bonhoeffer, F. (1987). Avoidance of posterior tectal membranes by temporal retinal axons. *Development* 101, 909–913.
- Zhang, J.H., Cerretti, D.P., Yu, T., Flanagan, J.G., and Zhou, R. (1996). Detection of ligands in regions anatomically connected to neurons expressing the Eph receptor Bsk: potential roles in neuron-target interaction. *J. Neurosci.* 16, 7182–7192.